AJNR

Experimental MR study of cerebral radiation injury: quantitative T2 changes over time and histopathologic correlation.

E Miot, D Hoffschir, C Alapetite, G Gaboriaud, D Pontvert, F Fetissof, A Le Pape and S Akoka

AJNR Am J Neuroradiol 1995, 16 (1) 79-85
http://www.ajnr.org/content/16/1/79

Experimental MR Study of Cerebral Radiation Injury: Quantitative T2 Changes over Time and Histopathologic Correlation

E. Miot, D. Hoffschir, C. Alapetite, G. Gaboriaud, D. Pontvert, F. Fetissof, A. Le Pape, and S. Akoka

PURPOSE: To use the pig brain as a large-animal model to examine the effects of high-dose single-fraction irradiation on MR images, T2 relaxation time, and histologic integrity. **METHODS:** A total of 24 Meishan pigs were studied: 20 irradiated animals and 4 unirradiated controls. A high dose was delivered to the right hemisphere of the animals, using a 12-MeV electron beam. Ten animals received 40 Gy at the 90% isodose, and 10 animals received 60 Gy. Quantitative measurement of T2 relaxation time was compared with qualitative analysis of T2-weighted images and histologic studies. **RESULTS:** Quantitative analysis revealed a reproducible increase of the T2 parameter within the irradiated areas. The T2 kinetic could be analyzed in two phases, which appeared before the visualization of ventricle compression, necrosis, and edema. The first is characterized by vascular inflammation and the latter by radiation necrosis and edema. Both are dose dependent. **CONCLUSION:** These results underline the ability of quantitative MR for early diagnosis of brain radiation lesions in vivo.

Index terms: Radiation, injuries; Brain, injuries; Brain, magnetic resonance; Animal studies

AJNR Am J Neuroradiol 16:79–85, January 1995

The success of radiation therapy depends not only on the dose required to treat tumors, but also on the dose that can be tolerated by the immediate surrounding tissues essential for the patient's survival. A substantial effort has been directed to overcome the negative effects of radiation therapy on the normal brain. Using stereotaxic techniques, dose localization has been considerably improved (1). Nevertheless, it is important to understand the radiation injury process to improve the understanding and follow-up of patients treated with radiation therapy.

Treatments to arrest the development of radiation therapy complications are not presently available; however, early detection of radiation injury to the normal brain could be a powerful tool to evaluate the harmlessness of different radiation therapy protocols.

Since magnetic resonance (MR) imaging became a diagnostic tool, the majority of the investigations have been anatomic ones. But MR lends itself to the study of functional tissue characteristics; one of the applications is the relaxation times measurements within specific regions of interest in organs. Discrete processes affecting the brain may not be visible on conventional MR scans but may still be detectable through quantitative analysis if significant alterations of relaxation times occur.

The purpose of this study was to investigate, after high-dose single-fraction irradiation, the radiation changes over time using quantitative T2 analysis for better understanding of radiation-induced MR changes and their histopathologic correlation.

Received November 16, 1993; accepted after revision April 25, 1994.

This work was supported by grant 6120 from the Association pour la Recherche sur le Cancer.

From the Laboratoire de Biophysique Cellulaire et RMN, Institut National de la Santé et de la Recherche Medicale, Tours, France (E.M., L.P., S.A.); CEA/DSV, Bruyères le Chatel, France (D.H.); Institut Curie, Paris, France (C.A., G.G., D.P.); and Laboratoire d'Anatomo-Pathologie, CHU Bretonneau, Tours, France (F.F.).

Address reprint requests to Elisabeth Miot, Laboratoire de Biophysique Cellulaire et RMN, Institut National de la Santé et de la Recherche Medicale, U316, 2bis, Blvd Tonnellé, 37032 Tours Cédex, France.

AJNR 16:79–85, Jan 1995 0195-6108/95/1601–0079

Materials and Methods

Animal Model

The Meishan pig was used as a large-animal model for this study. A total of 24 castrated male pigs (6 weeks old, 8 kg) were studied: 20 irradiated animals and 4 unirradiated controls. All animals were kept in an animal housing facility and were fed pig chow and given water ad libitum.

All animals were anesthetized with 25 mg/kg pentobarbital sodium and 3 mg/kg xylazine hydrochloride (Rompun) for the irradiation procedure. Pigs were placed in a prone position, and the electron beam port was positioned over the dorsal surface of the right hemisphere. A 40 × 35-mm port was used for beam delivery to the right hemisphere.

The skin surface dose was calculated to obtain an average brain dose at 2-cm depth (90% isodose). Pigs were irradiated with a 12-MeV electron beam at a rate of 2 Gy/min. Ten animals received single doses of 40 Gy at the 90% isodose, 10 animals received 60 Gy, and 4 pigs were used as controls.

The facilities and practices were in accordance with European Community guidelines for experimentation on animals.

MR Scanning

In vivo MR scans were performed on anesthetized animals using a 2.35-T proton-imaging system. Examinations were conducted using a 20-cm "bird cage resonator." At the beginning of each experiment, sagittal locator scans were acquired to facilitate a reproducible location of the coronal sections from the cerebellum to the olfactory bulbs of the animals. Spin-echo T2-weighted coronal scans were performed using 3000/30, 60, 90, 120, 150, 180/1 (repetition time/echo time/excitations). All images were obtained using a 256 × 256 matrix and a 20-cm field of view resulting in a 780-μm pixel size. Each coronal section was 5 mm thick with a 2.5-mm intersection spacing. Ten coronal sections were obtained. The examination procedure took about 40 minutes.

Qualitative analyses of the MR images were performed to detect general morphologic pathology. Quantitative measurement of T2 values was done using techniques previously described (2–4). Three selected regions of interest were placed within each of the irradiated and the contralateral hemispheres (Fig 1). These three regions had each received different doses from the beam: the first one at the 90% isodose (region A), the second one at the 70% isodose (region B), and the third one at the 40% isodose (region C). These regions of interest were represented by a circle, 3 pixels minimum in diameter, corresponding to a surface of 4 mm^2. The SD for T2 measurement was 5%. A region of interest chosen in the unirradiated cheek muscle was used as an internal control to normalize for any variation of our relaxation time–measuring technique.

For each dose, a T2 ratio, R, was calculated: R = T2 after irradiation/T2 before irradiation. R values were averaged for each group of animals. Average curves were plotted: T2 ratio evolution as a function of time after radiation therapy, for each region of interest. MR studies were performed at the following times: before irradiations, every 2 days during the 15 days after the treatment, and then at weekly intervals.

Fig 1. Diagram depicting the regions of interest of a coronal brain section studied with T2 relaxation time measurements.

Histology

Histologic examination was performed on pig brains at the following dates: 9, 25, 70, 160, and 180 days after the 40-Gy irradiation; 15, 85, 110, and 130 days after the 60-Gy irradiation; and for the control animals at 120, 150, 180, and 275 days of age. Evans blue (7 mL/kg) 2% solution in 9% saline (5) was infused into the jugular veins of the pigs 24 hours before killing them and removing the brains.

Pigs were killed with lethal overdoses of sodium pentobarbital. Animals were perfused with 10% formalin to ensure uniform fixation. The brains were removed and placed in formalin before being blocked for histologic sectioning and staining. All the brains were then embedded in paraffin, and 5-μm coronal sections were cut from the cerebellum to the olfactory bulbs.

Selected regions to correspond to the coronal MR sections were stained using hematoxylin and eosin and Luxol fast blue to detect general morphologic pathology and regions of demyelination and axonal injury. Microscopic specimens were evaluated for sites of tissue necrosis, demyelination, vessel wall thickening, gliosis, calcification, and hemorrhage. Alterations in the blood-brain barrier have been evaluated by Evans blue coloration on each side of the brain. The sections were also examined for gross anatomic changes such as ventricular compression and tissue swelling.

Results

One week after irradiation all the irradiated animals lost hair on the beam entrance impact. No differences of weight could be noted between the control and irradiated animals during all the months of monitoring.

We observed that all irradiated animals were sleepy during the 2 months after treatment. A loss of appetite, locomotor ataxia, and coordination and equilibrium difficulties appeared 6 months after a 40-Gy dose and 4 months after a 60-Gy dose.

MR Studies

Quantitative Analysis: Relaxation Times. The cerebral T2 values of the unirradiated animals were observed to be constant over time (results not shown). The interindividual variation was less than 10% for the determination of average R. We observed three different T2 phenomena within the irradiated areas: a transient early spike (phase I), an initial prolonged T2 increase (phase II), and a second prolonged T2 increase (phase III).

For the 40-Gy dose, Figure 2 shows R curves of 90% (Fig 2A), 70% (Fig 2B), and 40% (Fig 2C) isodose and equivalent contralateral regions of interest. (For better legibility, error bars are not plotted; in all these cases, the interindividual variation was less than 10%.)

After phase I at 2 days after irradiation, we observed a first long-lasting increase (phase II) in the R curve of 31%, from the 30th day to the 90th day after irradiation. Phase III began on the 110th day after the treatment and closed the curve with another increase of R up to 40% at day 190.

For the 60-Gy dose, Figure 3 shows the R curves of the 90% (Fig 3A), 70% (Fig 3B), and 40% (Fig 3C) isodose and equivalent contralateral regions of interest. The interindividual variation was less than 10%. We also observed a phase I and a phase II with increasing R up to 42%, from the 4th to the 45th day after irradiation. Phase III started 75 days after radiation treatment and ended at approximately 110 days with this second increase of R parameter up to 65%.

Examinations of Figures 2 and 3 revealed that the T2 ratio kinetic could be split in two long-lasting phases (phase II and phase III), whatever the dose was. Ventricular compression was seen early but after phase II. The hyperintense T2 parenchymal lesions were seen only after the onset of phase III. We also observed that the R increase rate was becoming greater when the radiation dose increased.

A

B

C

Fig 2. R curves of irradiated and contralateral regions of interest of the pig brain, as a function of time after radiation therapy with 40 Gy (12 MeV, electron beam). (For better legibility, error bars are not plotted; in all these cases, the interindividual variation was lower than 10%.)

A, Curve of 90% isodose region of interest (region A). *B,* Curve of 70% isodose region of interest (region B). *C,* Curve of 40% isodose region of interest (region C). The + line indicates irradiated region of interest; − line, contralateral region of interest.

A

B

C

Fig 3. R curves of irradiated and contralateral regions of interest of the pig brain, as a function of time after radiation therapy with 60 Gy (12 MeV, electron beam). (For a better legibility, error bars are not plotted; in all these cases, the interindividual variation was lower than 10%).

A, Curve of the 90% isodose region of interest (region A).

B, Curve of the 70% isodose region of interest (region B).

C, Curve of the 40% isodose region of interest (region C). The + line indicates irradiated region of interest; − line, contralateral region of interest.

Fig. 4. Greater R values of phase II and phase III as a function of the effective dose received.

The R average curves of regions of interest situated on the 70% isodose (region B) and 40% isodose (region C) revealed also a dose-dependent phenomenon for equivalent isodoses; however, the timing of this phenomenon was dependent only on the maximal dose received.

The greater R values of phase II and phase III of the curves have been plotted as a function of the dose (Fig 4). In the range of the investigated doses (ie, from 17 to 60 Gy), the greater R values seemed to be proportional to the effective dose received. This underlines the reliability and dose dependence of T2 relaxation time evolution after radiation therapy. Nevertheless, for a maximal dose received of 40 Gy, the R average curve for the 40% isodose-irradiated region of interest (region C) is not significantly different from the R average curve of the contralateral region of interest (Fig 2C).

Qualitative Studies. All unirradiated animals were neurologically normal and did not show any abnormalities on the MR scans.

The first radiation-induced MR anatomic change was the compression and occlusion of the irradiated lateral ventricle. This appeared in the irradiated hemisphere, on T2-weighted images after phase II: on the 90th (±10) day after irradiation for the 40-Gy dose; and on the 30th (±10) day after the treatment for the 60-Gy dose.

The second radiation-induced MR anatomic change was characterized by an increase of the signal intensity of the periventricular gray and white matter on T2-weighted images. This appeared in the irradiated hemisphere on T2-weighted images after phase III (Fig 5): on the 150th (±10) day for the 40-Gy dose; and on the

Fig 5. Coronal T2-weighted image of the pig brain at 150 days after irradiation with 40 Gy (12 MeV, electron beam). This MR scan showed increased signal intensity in the periventricular gray and white matter (*arrow*), suggesting the presence of edema and necrosis.

110th (±10) day for the 60-Gy dose. This visible signal change has been correlated with the detection of edema and necrosis on the corresponding histologic slices.

Histology

All unirradiated animals were neurologically normal and did not show any abnormalities on the histologic slices. The alterations observed with MR in irradiated animals have been correlated with histologic investigations (results not shown).

Initially, macrophage inflammation and vessel wall thickening were observed. Early histopathologic analysis reflected a vascular and glial mechanism of injury leading to a spreading vasogenic edema. Endothelial damages appeared on histologic slices from brain excised at 25 days after a 40-Gy dose and at 15 days after a 60-Gy dose.

Late changes at the 40-Gy dose included edema and necrosis detected in the regions of intense signal on T2-weighted images. The centers of the lesions were situated in the ventricle wall and in the thalamus.

Hemorrhages could be traced in the cerebral tissue, especially in the caudate nucleus, the central gray nuclei, and the meninges. Other radiation-induced damages included calcification, thrombosis, and nervous tissue disorganization.

Evans blue penetrated into the irradiated hemisphere 150 days after irradiation. Demyelination could be traced from the 120th day after treatment. Ventricle compression appeared 90 days after irradiation.

At the 60-Gy dose, regions of edema and necrosis appeared 120 days after the radiation treatment. Lesion location was traced in the ventricle wall and the thalamus. Many hemorrhages were detected in the cortex, the caudate nucleus, the thalamus, and the meninges.

An extension of the lesions to the hippocampus has been observed with a greater loss of pyramidal cells. After 120 days of irradiation, the Evans blue spots in the white and gray matter became larger. We observed a demyelination and ventricular compression 60 days after irradiation.

Discussion

The first MR description of radiation-induced lesions (6) included five patients with diffusely increased signal in the deep periventricular white matter on T2-weighted images and no focal abnormalities. Such observations revealed higher relaxation times for radiation-induced lesions than for normal white matter.

Constine et al (7) reported periventricular white matter changes on MR scans in all irradiated brains. MR scanning demonstrates radiation-induced changes accompanying blood-brain-barrier disruptions in the deep white matter. The MR abnormalities in cats consisted of high-intensity areas on long-repetition-time/long-echo-time images, which were associated with gadopentetate dimeglumine enhancement on T1-weighted inversion-recovery images, after a 50-Gy dose to a 1.5×1.5-cm^2 vertex portal (8).

Focal and diffuse high signal intensity in the white matter are generally accepted findings on T2-weighted spin-echo MR images after radiation therapy (9, 10). The degree and location of high-signal-intensity areas showed a close relationship with clinical symptoms and signs. The incidence of white matter changes increased with the dose of irradiation and time after therapy. (11).

From these experiments, we can summarize the following observations: A high-dose single-fraction irradiation induces an increase of the T2 relaxation time within the different regions of interest in the brain. After an immediate and transient spike of T2 after irradiation (phase I), T2 increase is a long-lasting and kinetic phe-

nomenon, which would reflect a developing disease. The T2 increase can be divided in two long-lasting phases.

Consistent results have been found between in vivo and histologic studies. The compression and occlusion of the irradiated ventricle starts after the first phase of T2 increase; edema and necrosis are detected by histologic studies after the second phase.

We found a dose dependence of T2 parameter between the two irradiation groups (40 and 60 Gy at 90%) and also within the same group (among the 90%, 70%, and 40% isodoses). The time dependence of T2 evolution depends only on the maximal dose received (90% isodose). This underlines the reliability and dose dependence of T2 relaxation time evolution after radiation therapy. The initial prolonged phase of T2 increase seems to be related to endothelial damages that could lead to the onset of a vasogenic edema and induce changes in water-diffusion patterns. Thus, T2 parameter seemed to be related to diffusion phenomenon in tissues. The second phase of T2 increase seems to be related to the development of edema.

We did not establish any correlation between the immediate and transient spike of T2 parameter (phase I) and any histopathologic phenomenon. We intend to perform a separate study, killing the animals 2 days after irradiation, to make an early pathologic analysis to better understand this transient T2 ratio spike.

Changes seen on relaxation times can reflect a wide spectrum of disease. The relaxation times are known to be closely correlated with the content of water and its dynamic structure in biological systems.

The special properties of hydration water molecules are averaged over all other water compartments in the system by diffusion and exchange, whereby they influence the relaxation time values. The T2 relaxation time is a sensitive monitor of water binding, particularly at low hydratation levels (12). The T2 of water bound to deoxyribonucleic acid, polynucleotides, and their complexes have been found to be very sensitive to changes in the structure of macromolecules in solutions induced by irradiation (13).

All stages of radiation injury do have in common chemical-bond breakages, molecular degradations, deoxyribonucleic acid breakages, and protein conformational changes. Vascular damage, edema, and swelling may lead to ischemic damage. Ball et al (14) observed that acute reactions are the result of transient vasogenic edema that may lead to mass effect and prolongation of relaxation parameters.

Many efforts have been made to obtain in vivo MR data on experimental animal models, particularly on experimental models of edema, ischemia, and infarction in the brain, which reproduce the mechanisms involved in brain radiation injury. Naruse and colleagues (15) and Bryan and colleagues (16) observed prolonged relaxation times after brain edema induced by cerebral ischemia and parallel changes in ischemic tissue water content. Naruse and colleagues (17) analyzed relaxation times during the course of experimental brain edema and cerebral infarction and observed that T2 values were prolonged after cold injury at the maximum period of edema.

From our experiments, the observed long-lasting elevated T2 values after irradiation are in keeping with the finding that the prolongation of T2 relaxation time is linearly correlated with water content (18) and seems to depict the constitutional change of edematous tissue (15). We also observed that the second phase of T2 increase appears just before the development of edema and necrosis.

The first long-lasting phase of T2 increase has been correlated with endothelial and vascular damages that could lead to alterations in diffusion. Recently a close correlation has been observed between ischemia, diffusion alteration, and prolonged T2 values in the brain, using diffusion-weighted images. Moseley and colleagues (19) compared T2 relaxation time and T2-weighted images with diffusion-weighted images and spectroscopy in an experimental model of regional cerebral ischemia; they found a correlation between both T2 relaxation time and diffusion-weighted images after 6 to 8 hours after a unilateral middle cerebral and bilateral carotid artery occlusion on a cat model. Ordidge and colleagues (20) observed that T2 values for ischemic brain tissue were elevated to approximatively 110% of control values. The ischemic T2 values also remained elevated 1 week after occlusion of the left carotid artery and the left middle cerebral artery in rats.

From our results, we hypothesize that the elevated and long-lasting T2 values of the irradiated regions in the brain may reflect a developing regional ischemia, possibly leading to an

infarcted area, such as those already observed by Benveniste and colleagues (21). These authors observed prolongation of T2 values in infarcted areas but also in noninfarcted areas. They introduced the hypothesis that the noninfarcted areas with elevated T2 values may reflect the ischemic penumbra (22). The ischemic penumbra could be seen using T2 calculated images.

Our results indicate that the observed prolonged elevated T2 values may reflect an initial diffusion abnormality caused vascular damage, which leads to alteration in water content and edema development. However, the T2 evolution after irradiation reflects a developing pathologic process.

Conclusion

The results reported here illustrate the usefulness of quantitative imaging to assess molecular tissue alterations to make early diagnosis of brain complications after radiation therapy. Regarding these results, we are able to perform kinetic analysis of the developing radiation injury process on the normal brain.

Using brain T2 relaxation time measurements, we can follow up the postradiotherapy period to detect earlier radiation-induced complications and locate the anatomic structures involved in this reaction. These results may help us understand better the natural history and the histopathologic events responsible for the observed T2 changes.

References

1. Philips TL. Early and late effects of radiation on normal tissues. In: Gutin PH, Leibel SA, Sheline GE, eds. *Radiation Injury to the Nervous System*. New York: Raven Press, 1991:37–67
2. Kjos BO, Ehman RL, Brant-Zawadzki M, Kelly WM, Norman D, Newton TH. Reproducibility of relaxation times and spin density calculated from routine MR imaging sequences: clinical study of the CNS. *AJNR Am J Neuroradiol* 1985;6:271–276
3. McFall JR, Wehrli FW, Breger RK, Johnson AJ. Methodology for the measurement and analysis of relaxation times in proton imaging. *Magn Reson Imaging* 1987;5:209–220
4. Tofts PS, Du Boulay EPGH. Towards quantitative measurements of relaxation times and other parameters in the brain. *Neuroradiology* 1990;32:407–415
5. Remler MP, Marcussen WH, Tiller-Borsich J. The late effects of radiation on the blood brain barrier. *Int J Radiat Oncol Biol Phys* 1986;12:1965–1969
6. Dooms GC, Hecht S, Brant-Zawadzki M, Berthiaume Y, Norman D, Newton TH. Brain radiation lesions: MR imaging. *Radiology* 1986;158:149–155
7. Constine LS, Konski A, Ekholm S, McDonald S, Rubin P. Adverse effects of brain irradiation correlated with MR and CT imaging. *Int J Radiat Oncol Biol Phys* 1988;15:319–330
8. Grossman RI, Hecht-Leavitt CM, Evans SM, et al. Experimental radiation injury: combined MR imaging and spectroscopy. *Radiology* 1988;169:305–309
9. Tsuruda JS, Kortman KE, Bradley WG, Wheeler DC, Van Dalsem W, Bradley TP. Radiation effects on cerebral white matter: MR evaluation. *AJNR Am J Neuroradiol* 1987;8:431–437
10. Curran WJ, Hecht-Leavitt C, Shut L, Zimerman RA, Nelson DF. Magnetic resonance imaging of cranial radiation lesions. *Int J Radiat Oncol Biol Phys* 1987;13:1093–1098
11. Nishimura R, Takahashi M, Morishita S, Sumi M, Uozumi H, Sakamoto Y. MR imaging of late radiation brain injury. *Radiat Med* 1992;10:101–108
12. Mathur-De-Vré R. Biomedical implications of the relaxation behaviour of water related to NMR imaging. *Br J Radiol* 1984;57: 955–976
13. Mathur-De-Vré R, Bertinchamps AJ, Berendsen HJC. The effects of γ irradiation on the hydratation characteristics of DNA and polynucleotides. I: an NMR study of frozen H_2O and D_2O solutions. *Radiat Res* 1976;68:197–214
14. Ball WS, Prenger EC, Ballard ET. Neurotoxicity of radio/chemotherapy in children: pathologic and MR correlation. *AJNR Am J Neuroradiol* 1992;13:761–776
15. Naruse S, Horikawa Y, Tanaka C, Hirakawa K, Nishikawa H, Yoshizaki K. Proton nuclear magnetic resonance studies on brain edema. *J Neurosurg* 1982;56:747–752
16. Bryan RN, Willcott MR, Schneiders NJ, Rose JE. NMR evaluation of stroke in the rat. *AJNR Am J Neuroradiol* 1983;4:242–244
17. Naruse S, Horikaw Y, Tanaka C, Hirakawa K, Nishikawa H, Yoshikazi K. Significance of proton relaxation time measurement in brain edema, cerebral infarction and brain tumors. *Magn Reson Imaging* 1986:4:293–304
18. Bederson JB, Bartkowski HM, Moon K, et al. Nuclear magnetic resonance imaging and spectroscopy in experimental brain edema in a rat model. *J Neurosurg* 1986;64:795–802
19. Moseley ME, Cohen Y, Mintorovitch J, et al. Early detection of regional cerebral ischemia in cats: comparison of diffusion- and T2-weighted MRI and spectroscopy. *Magn Reson Med* 1990;14: 330–346
20. Ordidge RJ, Helpern JA, Knight RA, Zhuangxian Q, Welch KMA. Investigation of cerebral ischemia using magnetization transfer contrast (MTC) MR imaging. *Magn Reson Imaging* 1991;9:895–902
21. Benveniste H, Cofer GP, Piantadosi CA, Davis JN, Johnson AG. Quantitative proton magnetic resonance imaging in focal cerebral ischemia in rat brain. *Stroke* 1991;22:259–268
22. Hakim AM. The cerebral ischemic penumbra. *Can J Neurol Sci* 1987;14:557–559

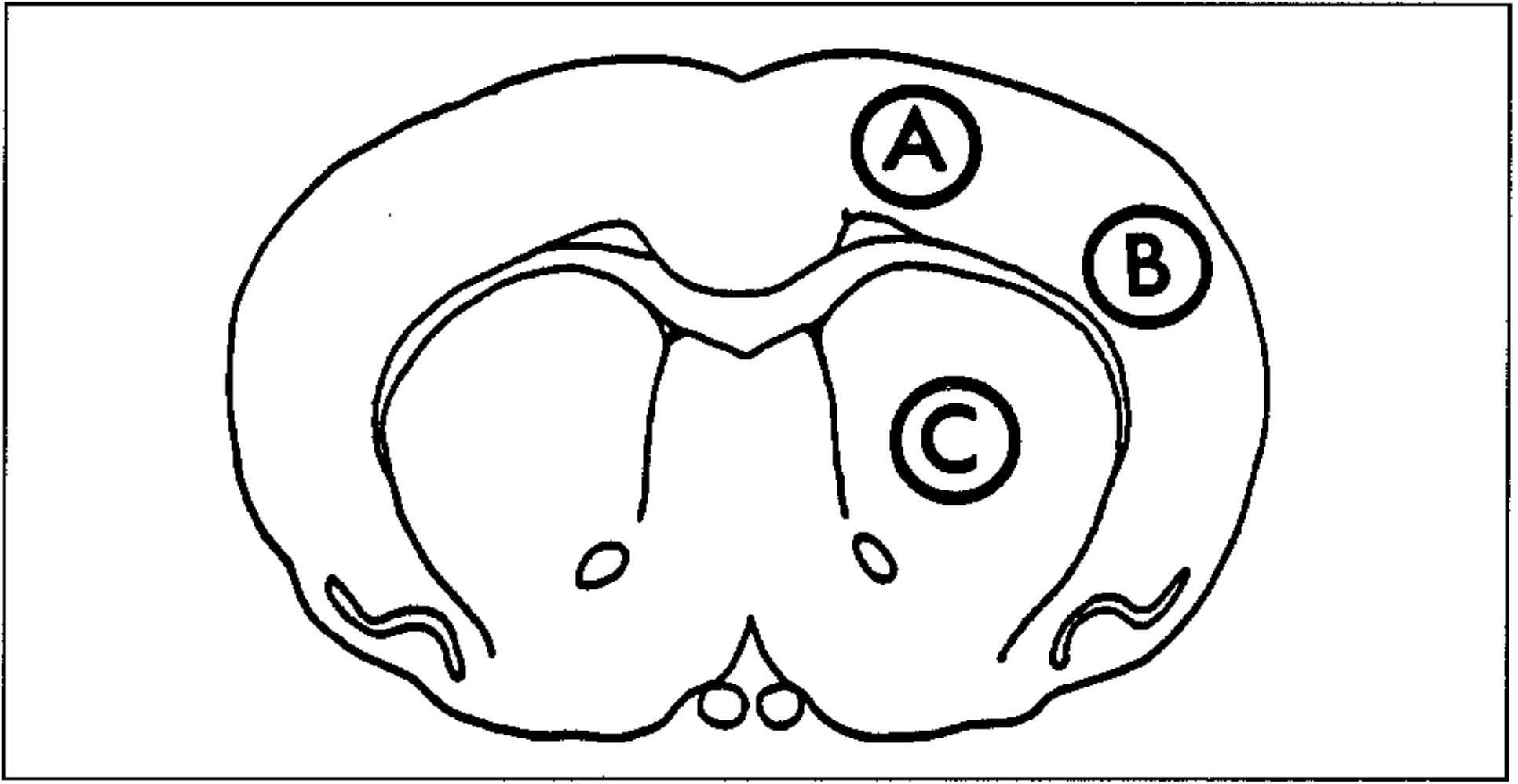
A
B
C

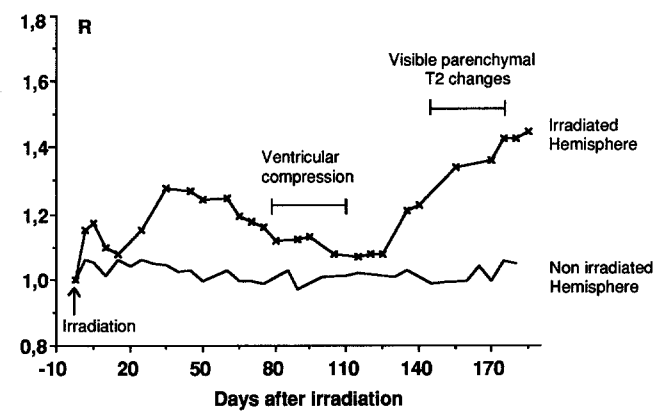
R
1,8
1,6
1,4
1,2
1,0
0,8
Visible parenchymal
T2 changes
Irradiated
Hemisphere
Ventricular
compression
Non irradiated
Hemisphere
Irradiation
-10
20
50
80
110
140
170
Days after irradiation

A

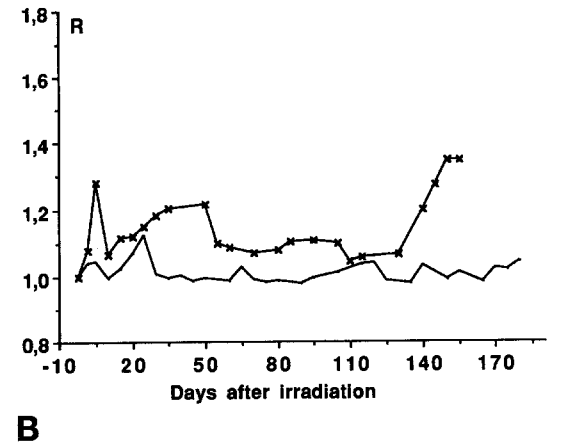
R
1,8
1,6
1,4
1,2
1,0
0,8
-10
20
50
80
110
140
170
Days after irradiation

B

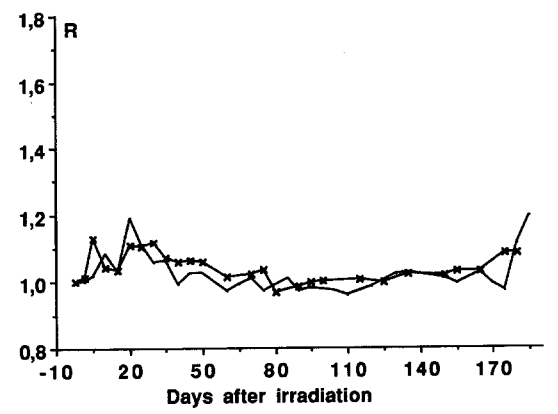
R
1,8
1,6
1,4
1,2
1,0
0,8
-10
20
50
80
110
140
170
Days after irradiation

C

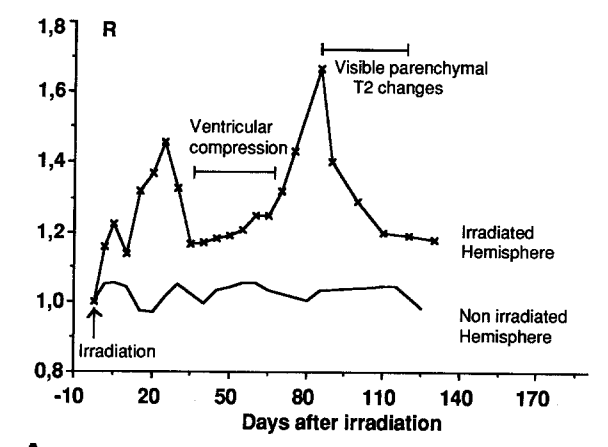
R
Visible parenchymal
T2 changes
Ventricular
compression
Irradiated
Hemisphere
Non irradiated
Hemisphere
Irradiation
1,8
1,6
1,4
1,2
1,0
0,8
-10
20
50
80
110
140
170
Days after irradiation

A

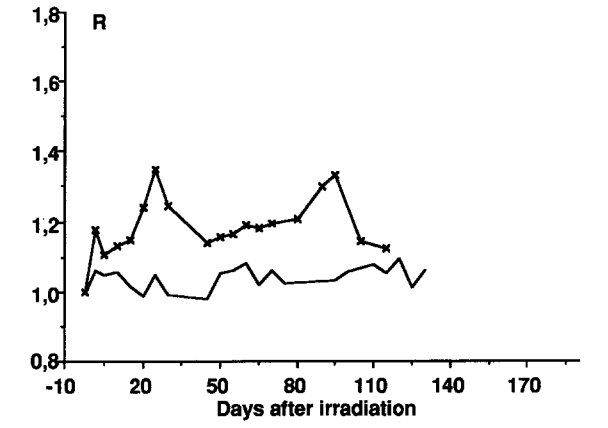
R
1,8
1,6
1,4
1,2
1,0
0,8
-10
20
50
80
110
140
170
Days after irradiation

B

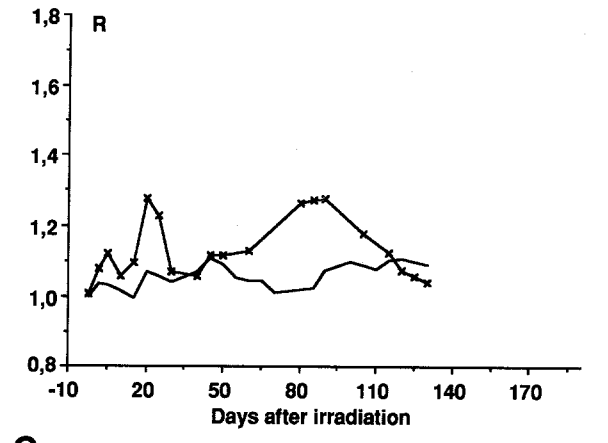
R
1,8
1,6
1,4
1,2
1,0
0,8
-10
20
50
80
110
140
170
Days after irradiation

C

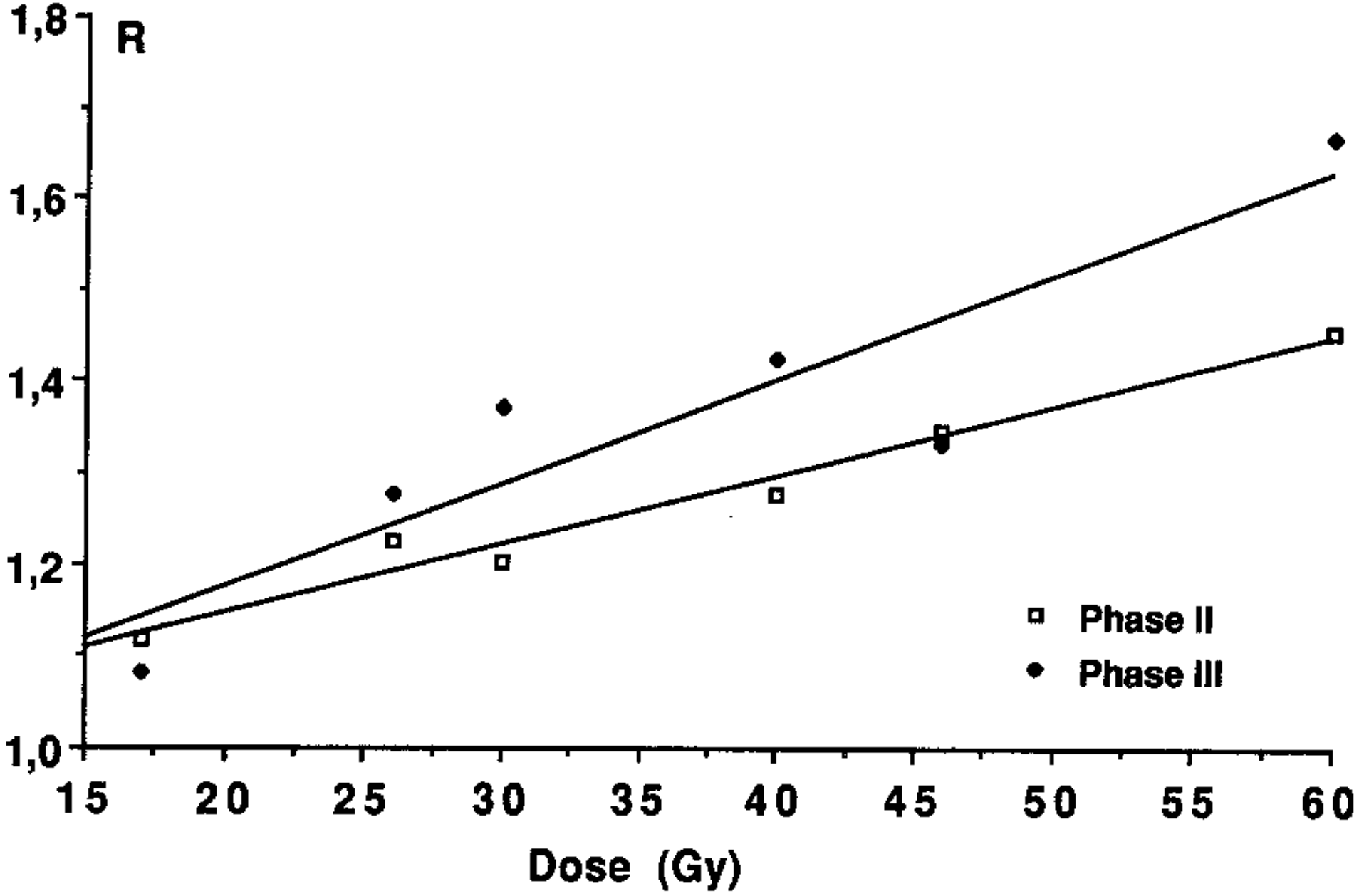
R
1,8
1,6
1,4
1,2
1,0
15
20
25
30
35
40
45
50
55
60
Dose (Gy)
Phase II
Phase III